Richter, LHJ, Menges, J, Wagmann, L, Brandt, SD, Stratford, A, Westphal, F, Flockerzi, V and Meyer, MR

In vitro toxicokinetics and analytical toxicology of three novel NBOMe derivatives - Phase I and II metabolism, plasma protein binding, and detectability in standard urine screening approaches studied by means of hyphenated mass spectrometry

Forensic Toxicology – accepted/uncorrected version

In vitro toxicokinetics and analytical toxicology of three novel NBOMe derivatives - Phase I and II metabolism, plasma protein binding, and detectability in standard urine screening approaches studied by means of hyphenated mass spectrometry

Lilian H. J. Richter[a], Julia Menges[a], Lea Wagmann[a], Simon D. Brandt[b], Alexander Stratford[c], Folker Westphal[d], Veit Flockerzi[e], and Markus R. Meyer[a]

[a] Department of Experimental and Clinical Toxicology, Institute of Experimental and Clinical Pharmacology and Toxicology, Center for Molecular Signaling (PZMS), Saarland University, 66421 Homburg, Germany

[b] School of Pharmacy and Biomolecular Sciences, Liverpool John Moores University, Byrom Street, Liverpool L33AF, UK

[c] Synex Synthetics BV, 6222NH, Maastricht, The Netherlands

[d] Section Narcotics/Toxicology, State Bureau of Criminal Investigation Schleswig-Holstein, 24116 Kiel, Germany

[e] Department of Experimental and Clinical Pharmacology, Institute of Experimental and Clinical Pharmacology and Toxicology, Center for Molecular Signaling (PZMS), Saarland University, 66421 Homburg, Germany

Contact

Markus R. Meyer, Department of Experimental and Clinical Toxicology, Institute of Experimental and Clinical Pharmacology and Toxicology, Center for Molecular Signaling (PZMS), Saarland University, Homburg, Germany

E-mail: markus.meyer@uks.eu

Abstract

Purpose

Toxicokinetic studies are essential in clinical and forensic toxicology to understand drug-drug interactions, influence of individual polymorphisms, and elimination routes, as well as to evaluate targets for toxicological screening procedures. An *N*-(2-methoxybenzyl)-substituted phenethylamines (NBOMe analogues) intake has been associated with severe adverse reactions including deaths. 1-(1-Benzofuran-5-yl)-N-[(2-methoxyphenyl)methyl]propan-2-amine (5-APB-NBOMe), 2-(8-bromo-2,3,6,7-tetrahydrobenzo[1,2-b:4,5-b′]difuran-4-yl)-N-[(5-chloro-2-ethoxyphenyl)methyl]ethan-1-amine (2C-B-FLY-NB2EtO5Cl), and 2-(8-bromo-2,3,6,7-tetrahydrobenzo[1,2-b:4,5-b′]difuran-4-yl)-N-[(2-methoxyphenyl)methyl]ethan-1-amine (2C-BFLY-NBOMe) are three emerging NBOMe analogues, which have encountered on the drugs of abuse market. So far, their toxicokinetic data are completely unexplored.

Methods

The study included mass spectrometry-based identification of phase I and II metabolites following exposure to the terminally differentiated human hepatocellular carcinoma cells (HepaRG). The determination of enzymes involved in the major phase I/II metabolic steps and determination of plasma protein binding (PPB) was done. Finally, the evaluation of the toxicological detectability by different hyphenated mass spectrometry techniques in standard urine screening approaches (SUSAs) was investigated.

Results

The compounds were extensively metabolized in HepaRG cells mainly via *O*-dealkylation, hydroxylation, glucuronidation, and combinations thereof. CYP1A2, 2D6, 2C8, 2C19, and 3A4, were involved in the initial reactions of all investigated compounds. Glucuronidation of the phase I metabolites – when observed - was mainly catalyzed by UGT1A9. The PPB of all compounds was determined to be > 85%. Only the high-resolution mass spectrometry-based SUSA allowed detection of all compounds in rat urine but only via metabolites.

Conclusions

The toxicokinetic data provided by this study will help forensic and clinical toxicologists to reliably identify these substances in case of abuse and/or intoxication and will allow them a thorough risk assessment.

KEYWORDS

NBOMe derivatives, HepaRG, metabolism, new psychoactive substances, LC-HRMS/MS

Introduction

The emergence of new psychoactive substances (NPS) has attracted the attention of various stakeholders concerned with the impact of drug abuse, social and individual harms and public health. The diverse nature of these particular substances adds significant challenges to forensic toxicology and groups include synthetic cannabinoid receptor agonists, synthetic cathinones, phenethylamines, and many others [1, 2]. A specific set of phenethylamines is represented by additional modification of the side chain nitrogen atom commonly referred to as *N*-(2-methoxybenzyl)-substituted phenethylamines (NBOMes), which have been associated with significant toxicity [3-10]. They are usually administrated via blotting papers [6] although drops for nasal application have also been reported [11]. Adverse effects include tachycardia, hypertension, and aggressive behavior [12] but other clinical features also associated with serotonergic toxicity have been reported including seizures, hyperthermia, and vasoconstriction [3]. NBOMes are highly potent agonists at various 5-HT receptor subtypes including $HT_{2A/2B/2C/1A}$ [3, 13]. 2-(8-Bromo-2,3,6,7-tetrahydrobenzo[1,2-*b*:4,5-*b*′]difuran-4-yl)ethan-1-amine (2C-B-FLY) belongs to a representative of the so-called "FLY" series that has been shown to be a potent 5-HT_{2A}-receptor agonist [e.g. 14, 15, 16]. In Europe, the detection of 2C-B-FLY has been reported to the European Monitoring Centre for Drugs and Drug Addiction (EMCDDA) first in 2007 [17]. Oral doses reported for some FLY compounds ranged from 0.5-20 mg [18]. 2-(8-Bromo-2,3,6,7-tetrahydrobenzo[1,2-*b*:4,5-*b*′]difuran-4-yl)-*N*-[(2-methoxyphenyl)methyl]ethan-1-amine (2C-B-FLY-NBOMe), i.e. the NBOMe derivative of 2C-B-FLY, has also been shown to activate the 5-HT_{2A} receptor [e.g. 14, 19] and thus suspected to result in psychoactive effects in humans. In more recent years, the detection of an unusual NBOMe derivative of 5-(2-aminopropyl)benzofuran (5-APB) was reported, namely 1-(1-benzofuran-5-yl)-*N*-[(2-methoxyphenyl)methyl]propan-2-amine (5-APB-NBOMe) [20-22]. The third NBOMe derivative featured in the present investigation was 2-(8-bromo-2,3,6,7-tetrahydrobenzo[1,2-*b*:4,5-*b*′]difuran-4-yl)-*N*-[(5-chloro-2-ethoxyphenyl)methyl]ethan-1-amine (2C-B-FLY-NB2EtO5Cl) that has to date not yet been described in the literature (all structures in Figure 1).

As NBOMe are known to be extensively metabolized [e.g. 23], metabolism studies are essential to understand drug-drug interactions, influence of individual polymorphisms, elimination routes, and for developing toxicological screening procedures [4-6, 23]. Therefore, the aims of the present study were tentative identification of their phase I and II metabolites by means of hyphenated high-resolution mass spectrometry (LC-HRMS/MS) after HepaRG exposure, determination of the isoenzymes involved in the major phase I and II metabolic steps, determination of plasma protein binding (PPB), and evaluation of their toxicological detectability by gas chromatography-mass spectrometry (GC-MS), liquid chromatography-mass spectrometry ($LC\text{-}MS^n$), and LC-HRMS/MS standard urine screening approaches (SUSAs) in rat urine after low dose administration.

Materials and methods

Chemicals, reagents, and biosamples

5-APB-NBOMe hydrochloride was provided by the Landeskriminalamt Schleswig-Holstein (Kiel, Germany), 2C-B-FLY-NBOMe hydrochloride was available from previous studies [24] and 2C-B-FLY-NB2EtO5Cl hydrochloride was from Synex Synthetics BV (Maastricht, The Netherlands). Isocitrate, isocitrate dehydrogenase, superoxide dismutase were obtained by Sigma-Aldrich (Taufkirchen, Germany), $NADP^+$ from Biomol (Hamburg, Germany), acetonitrile (LC-MS grade), ammonium formate (analytical grade), formic acid (LC-MS grade), methanol (LC-MS grade), and all other chemicals and reagents (analytical grade) from VWR (Darmstadt, Germany). Supersomes containing 1 nmol/mL of human cDNA-expressed cytochrome P450 (CYP) 1A2, CYP2A6, CYP2B6, CYP2C8, CYP2C9, CYP2C19, CYP2D6, CYP2E1 (2 nmol/mL), CYP3A4, CYP3A5 (2 nmol/mL), FMO3 (5 mg protein/mL), or 5 mg protein/mL of human cDNA-expressed UDP-glucuronyltransferase (UGT) 1A1, UGT1A3, UGT1A4, UGT1A6, UGT1A7, UGT1A8, UGT1A9, UGT1A10, UGT2B4, UGT2B7, UGT2B10, UGT2B15, UGT2B17, and control Supersomes without UGT activity (UGT control), and pooled human liver microsomes (pHLM, 20 mg microsomal protein/mL), UGT reaction mixture solution A (25 mM UDP-glucuronic acid), and UGT reaction mixture solution B (250 mM Tris-HCl, 40 mM $MgCl_2$, and 0.125 mg/mL alamethicin) were obtained

from Corning (Amsterdam, The Netherlands). The enzymes were aliquoted, snap-frozen in liquid nitrogen, and stored at -80 °C until use. Two-chambered Centrifree ultrafiltration devices were purchased from Merck Milipore (Darmstadt, Germany). Fresh human plasma samples were obtained from a local blood bank. Cryopreserved, differentiated HepaRG cells, 96-well plates coated with type I collagen, GlutaMAX, Williams Medium E, and supplement HPRG670 were obtained from Life Invitrogen (Darmstadt, Germany).

In vitro metabolism by HepaRG

According to Richter et al. [25], differentiated human hepatocellular carcinoma HepaRG cells at day 0, 4 h after cell seeding were used. The cells were treated under sterile conditions using a laminar flow bench class II (Thermo Scientific Schwerte, Germany) and maintained in an incubator (Binder, Tuttlingen, Germany) at 37°C with 95 % air humidity and 5 % CO_2 atmosphere. All given concentrations are final concentrations. The cells were seeded in a density of 72,000 cells/well (a 100-µL aliquot cell suspension per well) in collagen-coated 96-well plates. Williams E medium supplemented with HPRG670, 100 U/mL penicillin, and 100 µg/mL streptomycin (thaw and seed medium) were used for the cell incubation. A 50-µL aliquot was removed 4 h after cell seeding from the plate and 50 µL thaw and seed medium containing 50 µM or 500 µM of the investigated compounds were added, resulting in a final concentration of 25 µM or 250 µM. Cells were incubated for 24 h. For analysis of metabolites, supernatants from the well plates were collected. A 50-µL aliquot each was precipitated using 50 µL acetonitrile containing 0.1 % formic acid, vortexed, cooled at -18°C for 30 min, and centrifuged for 2 min at 18,407 x *g*. Afterwards, 50 µL of the supernatant was transferred to an autosampler vial. A 1-µL aliquot was injected onto the LC-HRMS/MS system as described below. Blank incubations without substrate and control incubations without cells were done. All incubations were done in triplicates.

Monooxygenases screening

For the monooxygenases screening, CYP1A2, CYP2A6, CYP2B6, CYP2C8, CYP2C9, CYP2C19, CYP2D6, CYP2E1, CYP3A4, CYP3A5 (75 pmol/mL each), FMO3 (0.25 mg protein/mL), or pHLM (1 mg protein/mL) as positive control were incubated with substrate for 30 min at 37 °C [26]. The following was added to the incubation: 90 mM phosphate buffer (pH 7.4), 5 mM Mg^{2+}, 5 mM isocitrate, 1.2 mM $NADP^{+}$, 0.5 U/mL isocitrate dehydrogenase, and 200 U/mL superoxide dismutase. For the isoenzymes CYP2A6 and CYP2C9 phosphate buffer was replaced with 90 mM Tris buffer (pH 7.4) according to manufactures recommendations. The reaction was started by addition of enzyme, and stopped by addition of 50 µL ice-cold acetonitrile. Afterwards the mixture was centrifuged for 2 min at 18,407 x *g*, 50 µL of the supernatant was transferred into an autosampler vial, and 1 µL was injected onto the LC-HRMS/MS system for analyzing described below. All incubations were done in duplicates.

UDP-glucuronyltransferase screening

For the UDP-glucuronyltransferase screening, a preincubation for 30 min at 37°C using the monooxygenase (75 pmol/mL each) responsible for initial phase I metabolic steps identified by monooxygenase activity screening was done using substrate (25 µM), 90 mM phosphate buffer (pH 7.4), 5 mM Mg^{2+}, 5 mM isocitrate, 1.2 mM $NADP^{+}$, 0.5 U/mL isocitrate dehydrogenase, and 200 U/mL superoxide dismutase. Thereafter, 25 µg/mL alamethicin (UGT reaction mixture solution B) and UGT1A1, UGT1A3, UGT1A4, UGT1A6, UGT1A7, UGT1A8, UGT1A9, UGT1A10, UGT2B4, UGT2B7, UGT2B10, UGT2B15, UGT2B17, or UGT control (0.75 mg protein/mL, respectively) were added and again preincubated for 10 min at 37°C. Glucuronidation reactions were started by adding 2.5 mM UDP-glucuronic acid (UGT reaction mixture solution A) and additionally incubated for 30 min at 37 °C with a final volume of 100 µL. The reactions were stopped by adding 50 µL ice-cold acetonitrile. After cooling for 30 min at -20 °C, the vials were centrifuged for 2 min at 18,407 x *g*. A 50-µL aliquot of the supernatant was transferred into an autosampler vial and 1 µL was injected onto the LC-HRMS/MS system as described below. All incubations were done in duplicates.

Determination of plasma protein binding (PPB)

According to published procedures [27, 28], two-chambered Centrifree ultrafiltration devices (molecular weight cut-off 30 kDa) were used. Three different concentrations of the investigated NPS were studied: 1, 2.5, and 5 µM (final concentrations). Fresh human plasma samples (450 µL) were spiked with 50 µL of the drug solution and incubated for 30 min at 37 °C (n=2). A 100-µL aliquot (global approach, GA) was transferred in a new reaction tube, mixed with 50 µL ice-cold acetonitrile, centrifuged for 2 min at 18,407 x *g*, and 100 µL of the supernatant was transferred in an autosampler vial (control). The remaining part of the incubation mixture was transferred into a Centrifree device and centrifuged at room temperature (22 °C) for 35 min at 1,600 x *g*. One hundred µL aliquots of the supernatant (SUP) and of the ultrafiltrate (UF) were mixed with 50 µL ice-cold acetonitrile. Supernatants were transferred into autosampler vials. All samples were analyzed by LC-HRMS/MS as described below. PPB was calculated as follows [27, 28].

$$(1)\ PPB, \% = \left(1 - \left(\frac{UF, \mu M}{GA, \mu M}\right)\right) \cdot 100\ \%$$

$$(2) GA, \mu M = \frac{(UF, \mu M + SUP, \mu M)}{2}$$

LogP values were calculated by ChemSketch 2016 1.1 (ACD/Labs, Toronto, Canada).

Quantification of the NBOMe derivative in the GA was used as control as the determined concentration should be the same as the calculated concentration (equation 2). Thanks to this comparison, an adsorption of the NBOMe derivative to the Centrifree device, especially the filter membrane, could be excluded.

LC-HRMS/MS apparatus for determination of phase I and II metabolites, monooxygenases and UDP-glucuronyltransferase screening, and PPB determination

According to published studies [5, 29], a Thermo Fisher Scientific (TF, Dreieich, Germany) Dionex UltiMate 3000 Rapid Separation (RS) UHPLC system with a quaternary UltiMate 3000 RS pump, an

UltiMate 3000 RS autosampler, and a TF Accucore phenyl-hexyl column (100 mm x 2.1 mm ID, 2.6 µm particle size) was used. The system was controlled by the TF Chromeleon software version 6.80 and the system was coupled to a TF Q-Exactive Plus equipped with a heated electrospray ionization II source (HESI-II). For calibrating the system, a Positive Mode Cal Mix (Supelco, Bellefonte, PA) at a flow rate of 3 µL/min using a syringe pump was used. The following conditions were applied: The mobile phase consisted of eluent A and eluent B. Eluent A consisted of 2 mM aqueous ammonium formate containing formic acid (0.1 %, *v/v*) and eluent B consisted of an ammonium formate solution with acetonitrile/methanol (50:50, *v/v*) containing formic acid (0.1 %, *v/v*) and water (1%, *v/v*). The gradient and the flow rate were adjusted as follows [9]: flow rate, 0.500 mL/min; gradient, 0-1.0 min 99% A, 1-10 min to 50 % A, 10-11.5 min hold 1% A, 11.5-13.5 min hold 99% A. HESI-II conditions were as described previously [30] and modified as follows: heater temperature, 320 °C; ion transfer capillary temperature, 320 °C; sheath gas, 60 arbitrary units (AU); auxiliary gas, 10 AU; spray voltage, 4.00 kV, positive mode, and S-lens RF level, 50.0. For MS, a positive electrospray ionization (ESI) full scan mode and a targeted MS^2 mode with an inclusion list containing the masses of interest as well activated pick others were used. For full scan data, the settings were as follows described: resolution, 35,000; automatic gain control (AGC) target, 1e6; maximum injection time (IT), 120 ms; scan range, *m/z* 150-900. For the MS^2 mode the settings were as follows described: 17,500; AGC target, 2e5; maximum IT, 250 ms; isolation window, *m/z* 1.0; normalized collision energy (NCE), 35 %. For data evaluation TF Xcalibur Qual Browser software version 2.2 SP 1.48 was used.

Detectability by standard urine screening approaches (SUSA)

According to previous studies [31], male Wistar rats (Charles River, Sulzfeld, Germany) were used corresponding to German law (Bundesrepublik Deutschland, 2013 Tierschutzgesetz, http://www.gesetze-im-internet.de/bundesrecht/tierschg/gesamt.pdf). The administration was done by gastric intubation using an aqueous suspension of the investigated compounds. Doses of 0.2 mg/kg body weight (BW) or 0.02 mg/kg BW were administrated. They were calculated as described by

Sharma et al. [32]. The rats were housed in metabolic cages for 24 h, having water ad libitum. Urine was collected separately from the feces over a 24-hour period. Blank urine samples were collected before drug administration to confirm the absence of interfering compounds. After collecting the urine samples were used directly analyzed and the remains stored at -20°C.

The SUSAs were performed as described previously [33, 34]. Briefly, for GC-MS, acidic hydrolysis, liquid-liquid extraction, and acetylation were performed before full scan GC-MS, AMDIS data evaluation, and library search. Urine was precipitated with acetonitrile for both liquid chromatography-mass spectrometry (LC-MS) approaches. The data of $LC\text{-}MS^n$ were evaluated using TF ToxID and library search [35] and the LC-HRMS/MS data using TF TraceFinder and library search [36].

Results and discussion

ESI^+ HRMS/MS fragmentation of 5-APB-NBOMe, 2C-B-FLY-NB2EtO5Cl, 2C-B-FLY-NBOMe, and their phase I and II metabolites

The measured accurate masses, relative intensities, calculated exact masses, elemental compositions, and mass deviations errors of the most abundant fragment ions of 5-APB-NBOMe, 2C-B-FLY-NB2EtO5Cl, 2C-B-FLY-NBOMe, and all their phase I and II metabolites tentatively identified using HepaRG cells are given in Table 1A-C. All metabolites were tentatively identified due to their accurate mass and fragmentation pattern as chemical synthetized standards were not commercially available. Seven phase I metabolites of 5-APB-NBOMe, four of 2C-B-FLY-NB2EtO5Cl, and five of 2C-B-FLY-NBOMe were tentatively identified. In addition, one phase II metabolite of 5-APB-NBOMe, two of 2C-B-FLY-NB2EtO5Cl, and one of 2C-B-FLY-NBOMe were found. In the following, fragmentation patterns of the parent compound and tentatively identified phase I metabolites are exemplarily discussed for 2C-B-FLY-NBOMe. Exceptions are mentioned separately. The *m/z* of the precursor ions (PI) and the fragment ions (FI) mentioned in the following text are based on the exact masses. The MS^2 spectra of 5-APB-NBOMe, 2C-B-FLY-NB2EtO5Cl, 2C-B-

FLY-NBOMe, and their metabolites detected or identified by LC-HRMS/MS SUSA are given in Figure 2 and 3. In terms of SUSA, "identified" means that an MS^2 spectrum was recorded and "detected" means that a MS^2 spectrum was not recorded but the *m/z* in the total ion chromatogram of the full-scan was present at the expected RT.

The MS^2 spectrum of 2C-B-FLY-NBOMe showed characteristic NBOMe FI and characteristic non-NBOMe FI. In case of 2C-B-FLY-NBOMe and 2C-B-FLY-NB2EtO5Cl, the non-NBOMe part was the FLY part and in case of 5-APB-NBOMe it was an amphetamine-type part. As already described by Casper et al. [23], the NBOMe part showed high abundant FIs and the non-NBOMe part showed lower abundant FIs, except for *O*-dealkylated metabolites. After *O*-dealkylation, the non-NBOMe part showed a very high abundance. The parent compound 2C-B-FLY-NBOMe with the PI at *m/z* 404.0848 was not the FI with the highest abundance. The FI at *m/z* 267.0011 was formed by the FLY part and showed a low abundance. This FI showed the intact FLY part with bromine. After a loss of bromine, the FI at *m/z* 188.0828 was formed. The most abundant FI at *m/z* 121.0645 was formed from the NBOMe part. From this FI the tropylium cation at *m/z* 91.0540 with a medium abundance was created by the loss of formaldehyde.

The phase I metabolite *O*-demethyl-2C-B-FLY-NBOMe (M15) with the PI at *m/z* 390.0692 showed FIs at *m/z* 267.0011, 188.0828, and 107.0489. The most abundant FI at *m/z* 267.0011 originated from the FLY part, as already mentioned, and abundances of the FIs reversed by a change of the NBOMe part. The FI at *m/z* 107.0489 corresponds to the *O*-demethylated NBOMe part. *O*-Demethyl-hydroxy-2C-B-FLY-NBOMe (M16) showed the same characteristic behavior as *O*-demethyl-2C-B-FLY-NBOMe (M15) for the abundances of the FIs. Due to the FI at *m/z* 264.9855, which originated from FI at *m/z* 388.0530 and additional elimination of water, the hydroxylation of M16 has to be located at the 2,3,6,7-tetrahydrobenzo[1,2-b:4,5-b']difuran part. The exact position of the hydroxy group could not be determined by fragmentation. Also the FI at *m/z* 186.0672 showed the double bond formed by elimination of water and could lead to stabilized by mesomerism.

Two monohydroxylated isomers were tentatively identified. M17 showed the FIs at *m/z* 264.9855 and 186.0672. As already described these fragment ions formed by a loss of water resulting in a

double bond and stabilizing effects due to mesomerism. The NBOMe part was not changed so the abundance of the FIs at *m/z* 264.9855 and 186.0672 was low but the most abundant FI at *m/z* 121.0645 was intact. Hydroxy isomer 2 (M18) most likely occurred after an aliphatic hydroxylation which showed the PI at *m/z* 420.0797. The FI at *m/z* 402.0692 formed via loss of water, which resulted in a double bond and the intact FIs at *m/z* 267.0011, 188.0828, and 121.0645. The FI at *m/z* 121.0645 showed the characteristic intact NBOMe part after loss of the FLY part, the FI at *m/z* 267.0011 showed the intact FLY component after loss of the NBOMe part, and the FI at *m/z* 188.0828 showed the FLY part after a loss of bromine.

One dihydroxy metabolite was tentatively identified. One of the hydroxy groups was located at the 2,3,6,7-tetrahydrobenzo[1,2-b:4,5-b']difuran nucleus which showed the characteristic FIs at *m/z* 264.9855 and 186.0672 originated from FI at *m/z* 418.0641. Dihydroxy 2C-B-FLY-NBOMe (M19) showed a loss of water which indicated an aliphatic hydroxylation and in addition the FIs at *m/z* 121.0645 and 91.0540 were intact. All spectra showed the bromine isotope shift of +1.9979 u. The phase I metabolites for 5-APB-NBOMe and 2C-B-FLY-NB2EtO5Cl showed similar fragmentation patterns. 5-APB-NBOMe showed additionally ring openings as one of the most abundant metabolites similar to what has been described for 5-APB [31]. The glucuronidated metabolites eliminated glucuronic acid (−176.0321 u) leading to similar spectra as those of the respective phase I metabolites. No *m/z* and MS^2 spectra of phase I metabolites conjugated with sulfate were identified meaning that no sulfates were formed or that their concentration was below the detection limit.

Proposed in vitro metabolic pathways

All metabolic steps following exposure of 5-APB-NBOMe to HepaRG are shown in Figure 4. The metabolic pathways of 5-APB-NBOMe could be summarized as follows: *O*-demethylation to *O*-demethyl-5-APB-NBOMe (M1), oxidative ring-opening of the benzofuran ring to 3-hydroxyethyl-4-hydroxy amphetamine-5-APB-NBOMe (M5) and 3-carboxymethyl-4-hydroxy amphetamine-5-APB-NBOMe (M7). Combinations of these metabolic steps result in 3-hydroxyethyl-4-hydroxy

amphetamine-*O*-demethyl-5-APB-NBOMe (M2) and 3-carboxymethyl-4-hydroxy amphetamine *O*-demethyl-5-APB-NBOMe (M4). 3-Hydroxyethyl-4-hydroxy amphetamine-5-APB-NBOMe glucuronide (M8) was the only tentatively identified phase II metabolite. Monohydroxylation formed hydroxy-5-APB-NBOMe (M3) as also one of the most abundant metabolites. Dihydroxy-5-APB-NBOMe (M6) was also detected.

The in vitro HepaRG metabolic pathways of 2C-B-FLY-NB2EtO5Cl (Figure 5) could be summarized as follows: Monohydroxylation to hydroxy-2C-B-FLY-NB2EtO5Cl isomer 1 (M10) and hydroxy-2C-B-FLY-NB2EtO5Cl isomer 2 (M11) as main metabolic steps, whereby a dihydroxylation to dihydroxy-2C-B-FLY-NB2EtO5Cl (M12) followed (most probable position of the hydroxy group is given in Figure 5). The most abundant metabolite M10 was additionally conjugated with glucuronic acid (M14). Also, an *O*-deethylation was detected (M9). A second glucuronide was tentatively identified as *O*-deethyl-hydroxy-2C-B-FLY-NB2EtO5Cl glucuronide (M13).

In vitro metabolic HepaRG pathways of 2C-B-FLY-NBOMe (Figure 6) were similar to those of 2C-B-FLY-NB2EtO5Cl. Monohydroxylation was one of the main metabolic steps, resulting in hydroxy-2C-B-FLY-NBOMe isomer 1 and 2 (M17, M18). Dihydroxylation was additionally observed (M19). Most probable position of the hydroxy group is given in Figure 6. Furthermore, *O*-dealkylation to *O*-demethyl-2C-B-FLY-NBOMe (M15) occurred and additionally a hydroxylation to *O*-demethyl-hydroxy-2C-B-FLY-NBOMe (M16). Only one phase II metabolite *O*-demethyl-2C-B-FLY-NBOMe glucuronide (M20) could be tentatively identified.

Monooxygenase screening

The monooxygenase isoenzymes catalyzing the initial metabolic steps of 5-APB-NBOMe, 2C-B-FLY-NB2EtO5Cl, and 2C-B-FLY-NBOMe are listed in Table 2. CYP1A2 was involved in *O*-dealkylation of all three derivatives. It was also catalyzing the hydroxylation of 5-APB-NBOMe and 2C-B-FLY-NBOMe. CYP2D6 was catalyzing hydroxylations of all three investigated NPS. CYP3A4 was only involved all metabolic phase I steps of 2C-B-FLY-NB2EtO5Cl. CYP2C8 was involved in hydroxylations of 5-APB-NBOMe and 2C-B-FLY-NBOMe and CYP2C19 involved in *O*-

dealkylation and hydroxylation of 2C-B-FLY-NB2EtO5Cl. The CYP enzyme catalyzing the ring opening of 5-APB-NBOMe could not be evaluated due to low metabolic formation rate in the initial monooxygenases activity screening.

UDP-glucuronyltransferase screening

The catalyzing UDP-glucuronyltransferase for glucuronidation of phase I metabolites are listed in Table 3. Glucuronidation was exclusively catalyzed by UGT1A9, except for 2C-B-FLY-NB2EtO5Cl, where UGT1A7 was additionally involved. The catalyzing UGT enzyme for glucuronidation of 3-hydroxyethyl-4-hydroxy amphetamine-5-APB-NBOMe (M5) could not be evaluated due to low metabolic formation rate of M5 in the initial monooxygenases activity screening.

Determination of plasma protein binding (PPB)

The lipophilicity of a compound is an important physicochemical property and associated with intermolecular interactions between plasma proteins and substrates [37, 38]. For all investigated NPS, the PPBs slightly increased by increasing plasma concentrations. These were unexpected findings as the PPB was expected to decrease with increasing plasma concentration [37, 38]. A possible explanation for this might be that the compounds exclusively bind to albumin or alpha-1-acid glycoprotein at low concentrations. At higher concentrations the investigated compounds may also bind to other plasma proteins such as globulins. The highest PPB was found for 2C-B-FLY-NB2EtO5Cl, which also had the highest logP value and thus the highest lipophilicity. 5-APB-NBOMe and 2C-B-FLY-NBOMe also showed a high PPB and also an increasing PPB by increasing concentrations. A list of the PPB at the different concentrations are given in Table 4.

Detectability using standard urine screening approaches (SUSA)

According to Sharma and McNeill [32] the administrated dosages were calculated to be 0.02 mg/kg BW (low dose I) and 0.2 mg/kg BW (low dose II) for toxicological detectability studies. The dosages

corresponded to human doses of 0.003 and 0.03 mg/kg BW, respectively, which are expected to be comparatively low [18, 13]. GC-MS, LC-MS^n, and LC-HRMS/MS SUSAs were used to investigate the toxicological detectability. Via GC-MS, neither parent compounds nor metabolites could be detected. All tentatively identified and detected metabolites using the LC-MS^n approach are listed in Table 5. No parent compounds were identified or detected and only two metabolites of 5-APB-NBOMe were found (M5 and M7). For 2C-B-FLY-NB2EtO5Cl no metabolites were detected. M17 was the only detected 2C-B-FLY-NBOMe metabolite. Using the LC-HRMS/MS approach, no parent compounds were detected. Spectra of 5-APB-NBOMe and all tentatively identified metabolites are given in Figure 2. In case of 2C-B-FLY-NB2EtO5Cl and 2C-B-FLY-NBOMe, metabolites were only detected but not identified. However, these metabolites are expected to be identified in intoxication cases and are therefore recommended as targets for detection of overdoses. Spectra of 2C-B-FLY-NB2EtO5Cl and 2C-B-FLY-NBOMe and all their detected metabolites are given in Figure 3. In summary, the LC-HRMS/MS SUSA seems to be the most promising procedure for a toxicological urine screening for 5-APB-NBOMe, 2C-B-FLY-NB2EtO5Cl, and 2C-B-FLY-NBOMe by using metabolites as screening targets.

Conclusions

The NPS 5-APB-NBOMe, 2C-B-FLY-NB2EtO5Cl, and 2C-B-FLY-NBOMe were found to be extensively metabolized in HepaRG cells mainly via *O*-dealkylation, hydroxylation, glucuronidation, and combinations thereof. Due to the structural similarity of the studied NPS, the same monooxygenase isoenzymes were involved in the initial metabolic reactions, namely CYP1A2, 2D6, 2C8, 2C19, and 3A4. Glucuronidation of the phase I metabolites was mainly catalyzed by UGT1A9 for all investigated compounds. The tentatively identified in vitro metabolites could be used as targets for urinary toxicological screening approaches. From the investigated SUSAs, only the HRMS/MS-based SUSA is expected to allow detection of an intake of low amounts but only in the form of their metabolites.

Acknowledgements

The authors like to thank Hans H. Maurer and Armin A. Weber for their support and fruitful discussion.

Compliance with ethical standards

Conflict of interest

The authors declare that they have no conflict of interest.

Ethical approval

This article does not contain any studies with human participants performed by any of the authors. The authors declare that the animal experiments have been conducted in accordance with all applicable institutional, national, or international guidelines for care and use of rats. Studies have been approved by an ethics committee (Landesamt für Verbraucherschutz, Saarbrücken, Germany).

References

[1] Evans-Brown M, Sedefov R (2018) Responding to new psychoactive substances in the European Union: early warning, risk assessment, and control measures. Handb Exp Pharmacol 252:3-49

[2] Tettey JNA, Crean C, Ifeagwu SC, Raithelhuber M (2018) Emergence, diversity, and control of new psychoactive substances: a global perspective. Handb Exp Pharmacol 252:51-67

[3] Halberstadt AL (2017) Pharmacology and toxicology of N-benzylphenethylamine ("NBOMe") hallucinogens. Current Topics In Behavioral Neurosciences 32:283-311

[4] Caspar AT, Brandt SD, Stoever AE, Meyer MR, Maurer HH (2017) Metabolic fate and detectability of the new psychoactive substances 2-(4-bromo-2,5-dimethoxyphenyl)-N-[(2-methoxyphenyl)methyl]ethanamine (25B-NBOMe) and 2-(4-chloro-2,5-dimethoxyphenyl)-N-[(2-methoxyphenyl)methyl]ethanamine (25C-NBOMe) in human and rat urine by GC-MS, LC-MS(n), and LC-HR-MS/MS approaches. J Pharm Biomed Anal 134:158-69

[5] Caspar AT, Helfer AG, Michely JA, Auwarter V, Brandt SD, Meyer MR et al. (2015) Studies on the metabolism and toxicological detection of the new psychoactive designer drug 2-(4-iodo-2,5-dimethoxyphenyl)-N-[(2-methoxyphenyl)methyl]ethanamine (25I-NBOMe) in human and rat urine using GC-MS, LC-MS(n), and LC-HR-MS/MS. Anal Bioanal Chem 407:6697-719

[6] Poklis JL, Dempsey SK, Liu K, Ritter JK, Wolf C, Zhang S et al. (2015) Identification of metabolite biomarkers of the designer hallucinogen 25I-NBOMe in mouse hepatic microsomal preparations and human urine samples associated with clinical intoxication. J Anal Toxicol 39:607-16

[7] Poklis JL, Nanco CR, Troendle MM, Wolf CE, Poklis A (2014) Determination of 4-bromo-2,5-dimethoxy-N-[(2-methoxyphenyl)methyl]-benzeneethanamine (25B-NBOMe) in serum and urine by high performance liquid chromatography with tandem mass spectrometry in a case of severe intoxication. Drug Test Anal 6:764-9

[8] Poklis JL, Raso SA, Alford KN, Poklis A, Peace MR (2015) Analysis of 25I-NBOMe, 25B-NBOMe, 25C-NBOMe and other dimethoxyphenyl-N-[(2-methoxyphenyl)methyl]ethanamine derivatives on blotter paper. J Anal Toxicol 39:617-23

[9] Richter LHJ, Flockerzi V, Maurer HH, Meyer MR (2017) Pooled human liver preparations, HepaRG, or HepG2 cell lines for metabolism studies of new psychoactive substances? A study using MDMA, MDBD, butylone, MDPPP, MDPV, MDPB, 5-MAPB, and 5-API as examples. J Pharm Biomed Anal 143:32-42

[10] Caspar AT, Meyer MR, Maurer HH (2018) Human cytochrome P450 kinetic studies on six N-2-methoxybenzyl (NBOMe)-derived new psychoactive substances using the substrate depletion approach. Toxicol Lett 285:1-8

[11] Ameline A, Farrugia A, Raul JS, Kintz P (2017) Retrospective demonstration of 25I-NBOMe acute poisoning using hair analysis. Curr Pharm Biotechnol 18:786-90

[12] Rose SR, Poklis JL, Poklis A (2013) A case of 25I-NBOMe (25-I) intoxication: a new potent 5-HT2A agonist designer drug. Clin Toxicol (Phila) 51:174-7

[13] Eshleman AJ, Wolfrum KM, Reed JF, Kim SO, Johnson RA, Janowsky A (2018) Neurochemical pharmacology of psychoactive substituted N-benzylphenethylamines: High potency agonists at 5-HT2A receptors. Biochem Pharmacol 158:27-34

[14] Heim R (2003) Synthese und Pharmakologie potenter 5-HT_{2A}-Rezeptoragonisten mit *N*-2-Methoxybenzyl-Partialstruktur. Entwicklung eines neuen Struktur-Wirkungskonzepts. Freie Universität Berlin, Germany.Ph.D. dissertation

[15] Monte AP, Marona-Lewicka D, Parker MA, Wainscott DB, Nelson DL, Nichols DE (1996) Dihydrobenzofuran analogues of hallucinogens. 3. Models of 4-substituted (2,5-dimethoxyphenyl)alkylamine derivatives with rigidified methoxy groups. J Med Chem 39:2953-61

[16] Halberstadt AL, Chatha M, Stratford A, Grill M, Brandt SD (2019) Comparison of the behavioral responses induced by phenylalkylamine hallucinogens and their tetrahydrobenzodifuran ("FLY") and benzodifuran ("DragonFLY") analogs. Neuropharmacology 144:368-76

[17] EMCDDA. EMCDDA–Europol 2007 Annual Report on the implementation of Council Decision 2005/387/JHA. In accordance with Article 10 of Council Decision 2005/387/JHA on information exchange, risk assessment and control of new psychoactive substances. EMCDDA, Lisbon.

http://www.emcdda.europa.eu/system/files/publications/503/2007_Implementation_report_281403.pdf2008.

[18] Noble C, Holm NB, Mardal M, Linnet K (2018) Bromo-dragonfly, a psychoactive benzodifuran, is resistant to hepatic metabolism and potently inhibits monoamine oxidase A. Toxicol Lett 295:397-407

[19] Ettrup A, Hansen M, Santini MA, Paine J, Gillings N, Palner M et al. (2011) Radiosynthesis and in vivo evaluation of a series of substituted ^{11}C-phenethylamines as 5-HT$_{2A}$ agonist PET tracers. European Journal of Nuclear Medicine and Molecular Imaging 38:681-93

[20] EMCDDA. EMCDDA–Europol 2014 Annual Report on the implementation of Council Decision 2005/387/JHA. In accordance with Article 10 of Council Decision 2005/387/JHA on the information exchange, risk assessment and control of new psychoactive substances. EMCDDA, Lisbon. http://www.emcdda.europa.eu/system/files/publications/1018/TDAN15001ENN.pdf2015.

[21] Westphal F, Girreser U, Waldmuller D (2016) Analytical characterization of four new ortho-methoxybenzylated amphetamine-type designer drugs. Drug Test Anal 8:910-9

[22] Liu C, Jia W, Qian Z, Li T, Hua Z (2017) Identification of five substituted phenethylamine derivatives 5-MAPDB, 5-AEDB, MDMA methylene homolog, 6-Br-MDMA, and 5-APB-NBOMe. Drug Test Anal 9:199-207

[23] Caspar AT, Westphal F, Meyer MR, Maurer HH (2018) LC-high resolution-MS/MS for identification of 69 metabolites of the new psychoactive substance 1-(4-ethylphenyl-)-N-[(2-methoxyphenyl)methyl] propane-2-amine (4-EA-NBOMe) in rat urine and human liver S9 incubates and comparison of its screening power with further MS techniques. Anal Bioanal Chem 410:897-912

[24] Wagmann L, Brandt SD, Stratford A, Maurer HH, Meyer MR (2019) Interactions of phenethylamine-derived psychoactive substances of the 2C-series with human monoamine oxidases. Drug Test Anal 11:318-24

[25] Richter LHJ, Herrmann J, Andreas A, Park YM, Wagmann L, Flockerzi V et al. (2018, submitted) Tools for studying the metabolism of new psychoactive substances for toxicological

screening purposes - A comparative study using pooled human liver S9, HepaRG cells, and zebrafish larvae.

[26] Wagmann L, Meyer MR, Maurer HH (2016) What is the contribution of human FMO3 in the N-oxygenation of selected therapeutic drugs and drugs of abuse? Toxicol Lett 258:55-70

[27] Mardal M, Gracia-Lor E, Leibnitz S, Castiglioni S, Meyer MR (2016) Toxicokinetics of new psychoactive substances: plasma protein binding, metabolic stability, and human phase I metabolism of the synthetic cannabinoid WIN 55,212-2 studied using in vitro tools and LC-HR-MS/MS. Drug Test Anal 8:1039-48

[28] Fung EN, Chen YH, Lau YY (2003) Semi-automatic high-throughput determination of plasma protein binding using a 96-well plate filtrate assembly and fast liquid chromatography-tandem mass spectrometry. J Chromatogr B Analyt Technol Biomed Life Sci 795:187-94

[29] Wagmann L, Brandt SD, Kavanagh PV, Maurer HH, Meyer MR (2017) In vitro monoamine oxidase inhibition potential of alpha-methyltryptamine analog new psychoactive substances for assessing possible toxic risks. Toxicol Lett 272:84-93

[30] Helfer AG, Turcant A, Boels D, Ferec S, Lelievre B, Welter J et al. (2015) Elucidation of the metabolites of the novel psychoactive substance 4-methyl-N-ethyl-cathinone (4-MEC) in human urine and pooled liver microsomes by GC-MS and LC-HR-MS/MS techniques and of its detectability by GC-MS or LC-MS(n) standard screening approaches. Drug Test Anal 7:368-75

[31] Welter J, Kavanagh P, Meyer MR, Maurer HH (2015) Benzofuran analogues of amphetamine and methamphetamine: studies on the metabolism and toxicological analysis of 5-APB and 5-MAPB in urine and plasma using GC-MS and LC-(HR)-MS(n) techniques. Anal Bioanal Chem 407:1371-88

[32] Sharma V, McNeill JH (2009) To scale or not to scale: the principles of dose extrapolation. Br J Pharmacol 157:907-21

[33] Maurer HH, Pfleger K, Weber AA. Mass spectral data of drugs, poisons, pesticides, pollutants and their metabolites. Weinheim: Wiley-VCH; 2016.

[34] Meyer MR, Lindauer C, Welter J, Maurer HH (2014) Dimethocaine, a synthetic cocaine analogue: studies on its in-vivo metabolism and its detectability in urine by means of a rat model and liquid chromatography-linear ion-trap (high-resolution) mass spectrometry. Anal Bioanal Chem 406:1845-54

[35] Maurer HH, Wissenbach DK, Weber AA. Maurer/Wissenbach/Weber MWW LC-MSn library of drugs, poisons, and their metabolites. 2nd ed. Weinheim, Germany: Wiley-VCH; 2018.

[36] Maurer HH, Meyer MR, Helfer AG, Weber AA. Maurer/Meyer/Helfer/Weber MMHW LC-HR-MS/MS library of drugs, poisons, and their metabolites. Weinheim, Germany: Wiley-VCH; 2018.

[37] Kratochwil NA, Huber W, Muller F, Kansy M, Gerber PR (2002) Predicting plasma protein binding of drugs: a new approach. Biochem Pharmacol 64:1355-74

[38] Kratochwil NA, Huber W, Muller F, Kansy M, Gerber PR (2004) Predicting plasma protein binding of drugs--revisited. Curr Opin Drug Discov Devel 7:507-12

Figures

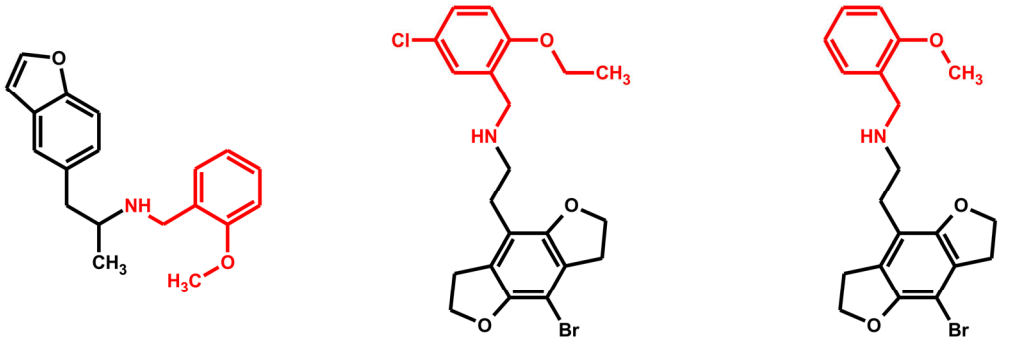

Figure 1. Structures of the investigated new psychoactive substances.

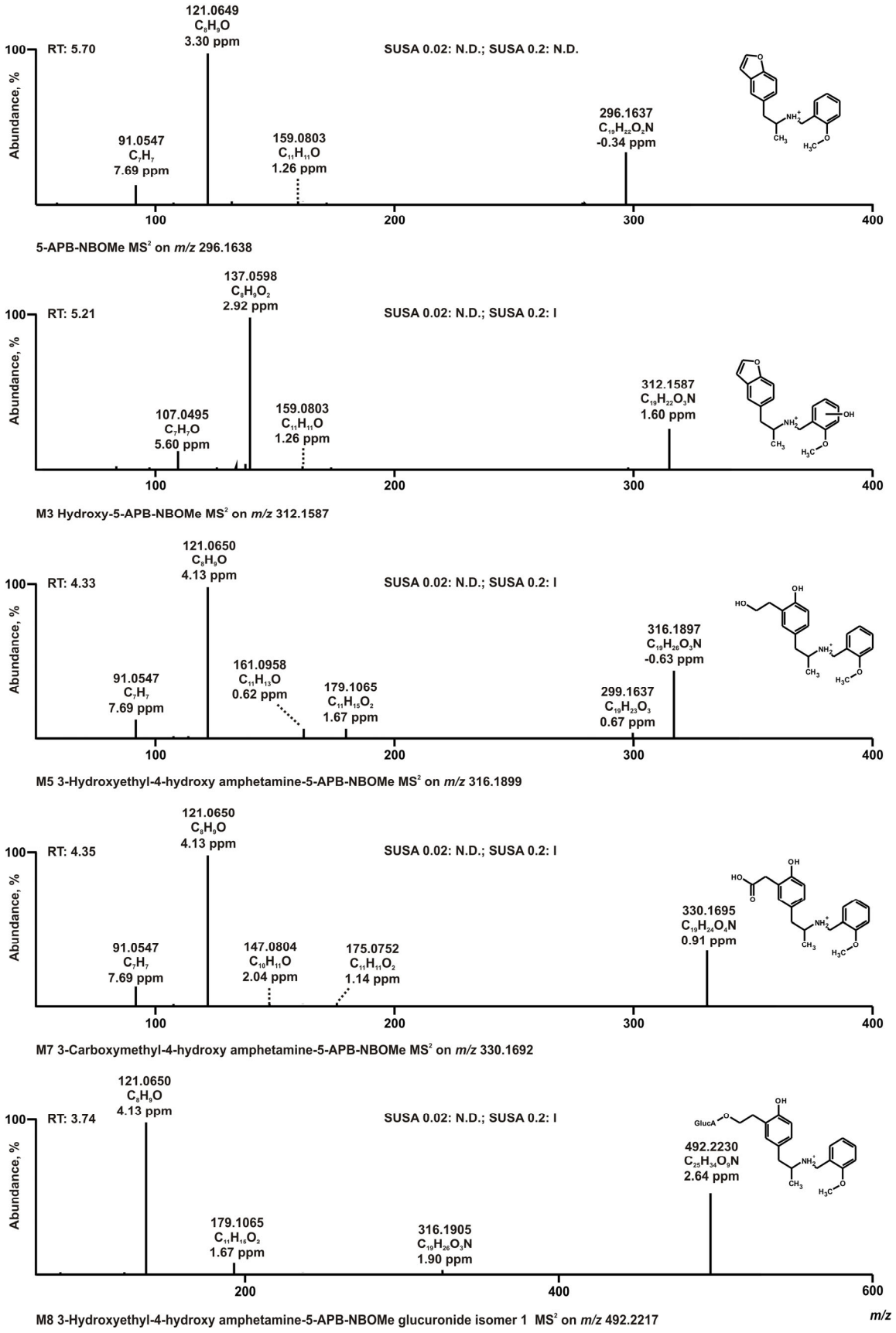

Figure 2. HRMS/MS spectra, structures, and predominate fragmentation patterns of 5-APB-NBOMe and its metabolites identified (I) by LC-HRMS/MS standard urine screening approach (SUSA) in very low dose (0.02 mg/kg body weight) and low dose (0.2 mg/kg body weight) rat urine (N.D. = not detected). Metabolites arranged according to precursor masses and retention times (RT).

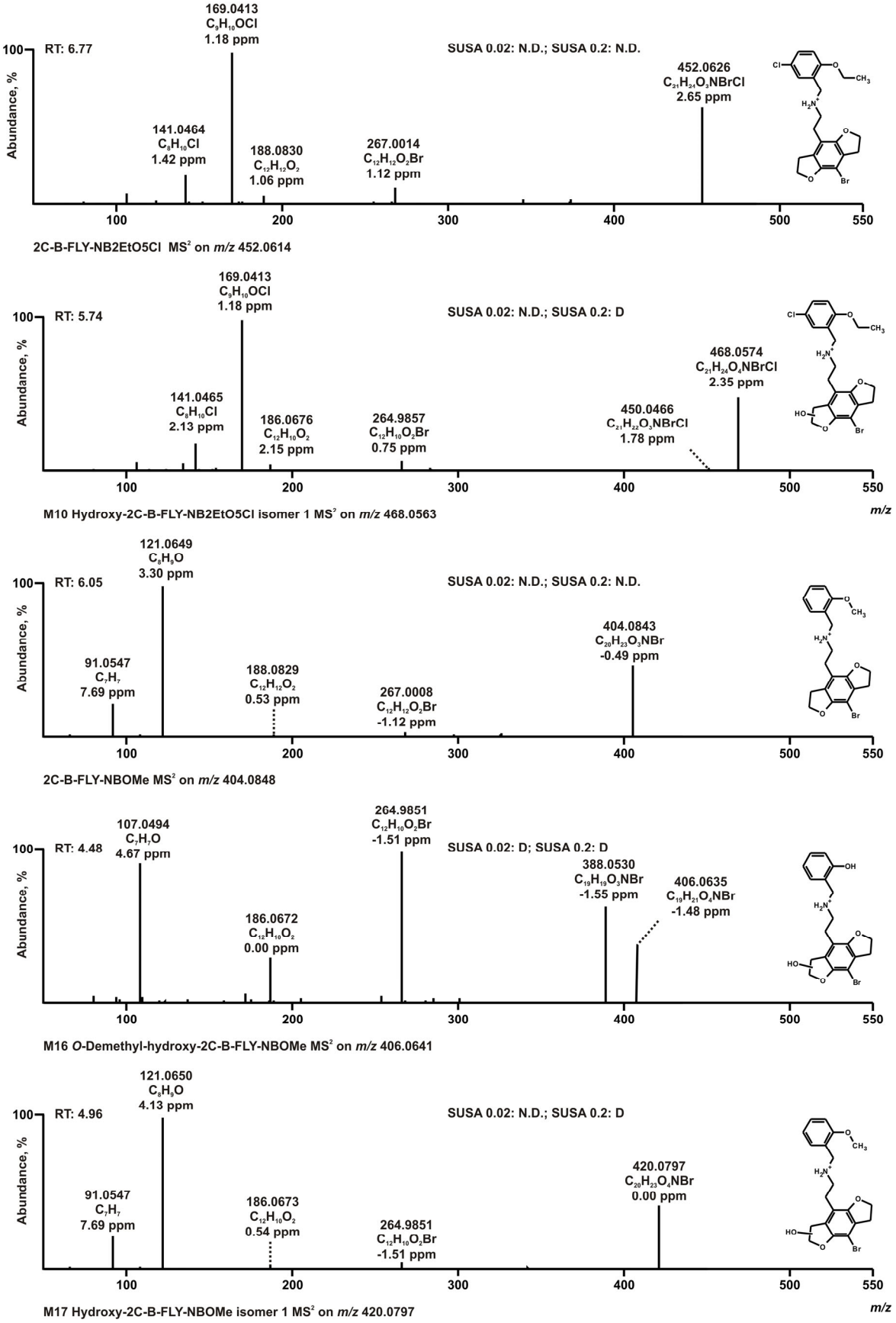

Figure 3. HRMS/MS spectra, structures, and predominate fragmentation patterns of 2C-B-FLY-NB2EtO5Cl, 2C-B-FLY-NBOMe, and their metabolites identified (I) or detected (D) by LC-HRMS/MS standard urine screening approach (SUSA) in very low dose (0.02 mg/kg body weight) and low dose (0.2 mg/kg body weight) rat urine (N.D. : not detected). Metabolites arranged according to precursor masses and retention times (RT).

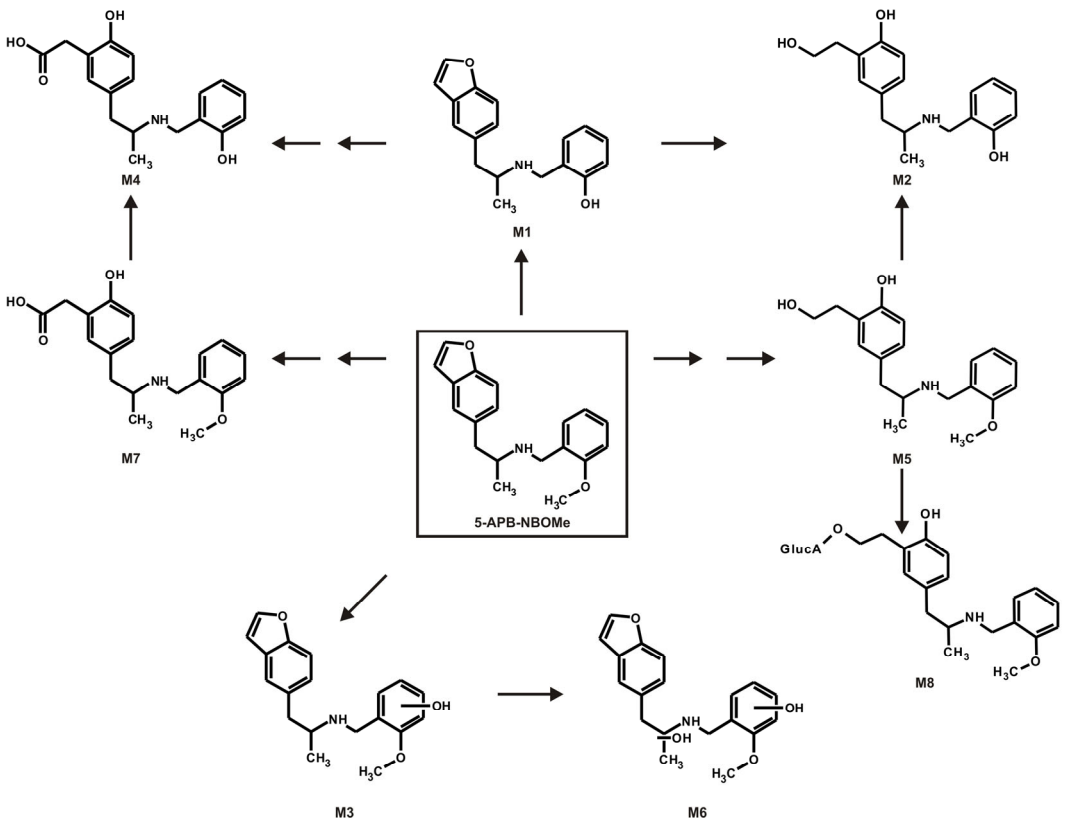

Figure 4. In vitro metabolic pathways of 5-APB-NBOMe identified using HepaRG cells by means of LC-HRMS/MS.

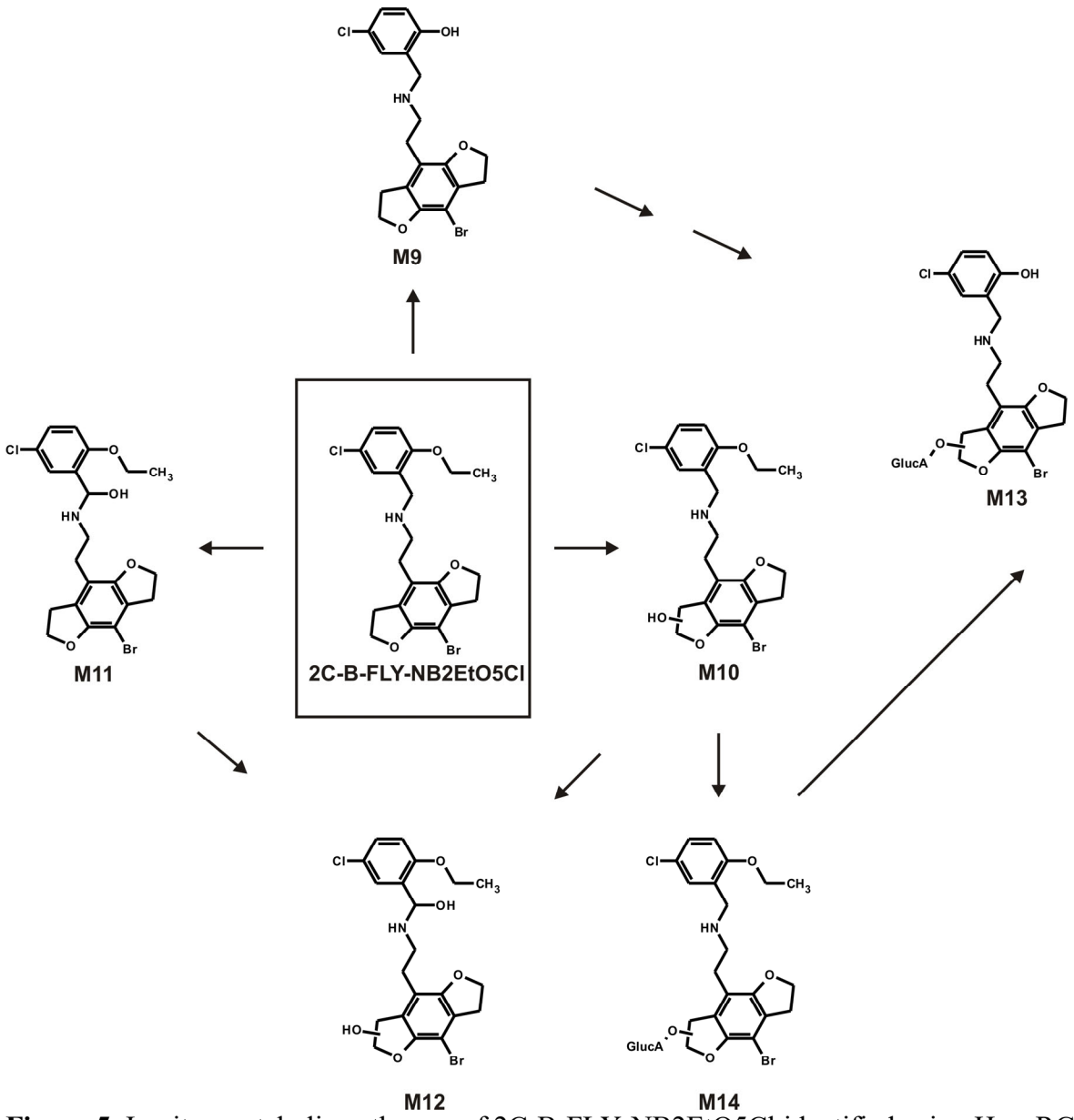

Figure 5. In vitro metabolic pathways of 2C-B-FLY-NB2EtO5Cl identified using HepaRG cells by means of LC-HRMS/MS.

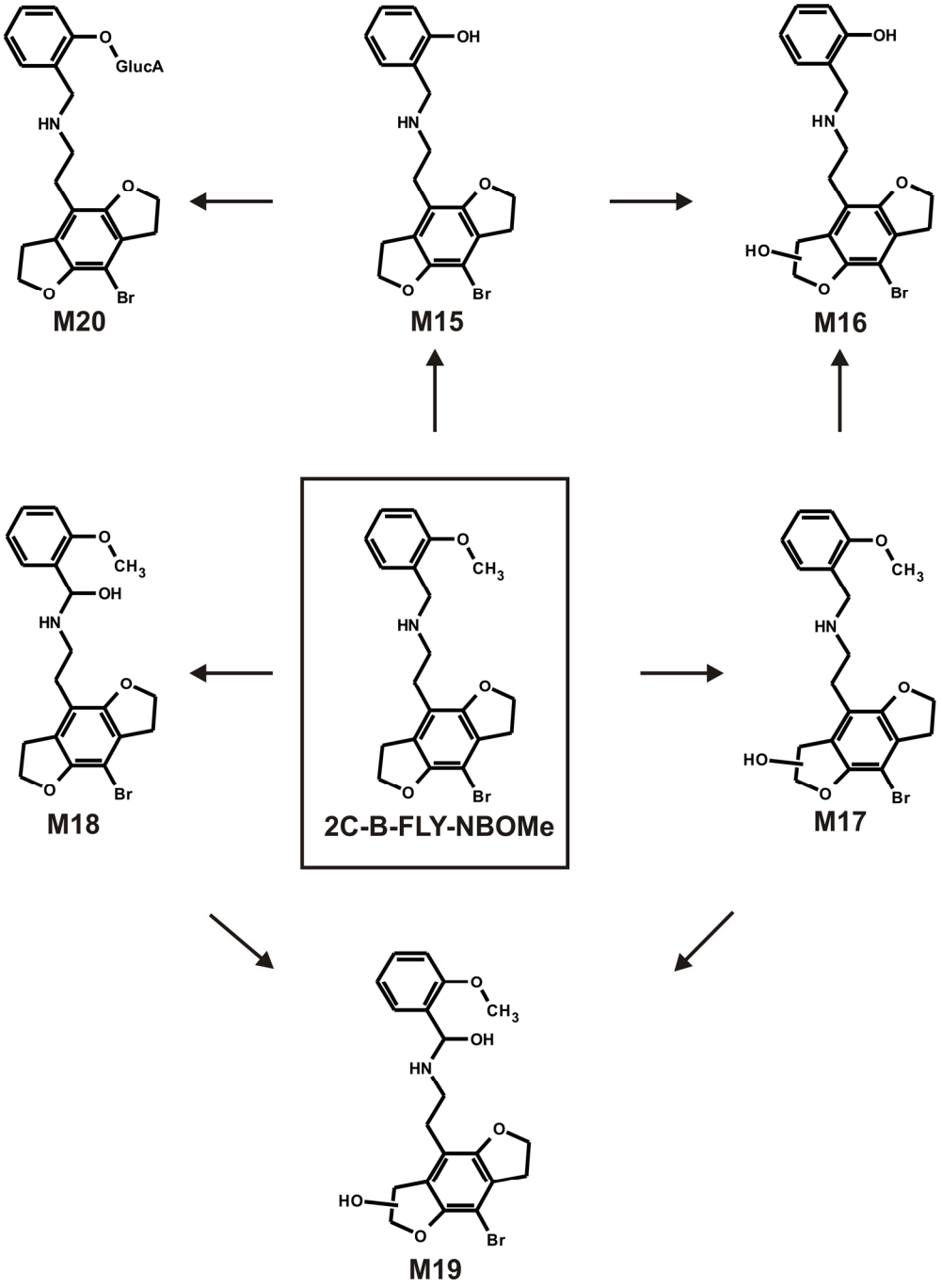

Figure 6. In vitro metabolic pathways of 2C-B-FLY-NBOMe identified using HepaRG cells by means of LC-HRMS/MS.

Table 1A. List of 5-APB-NBOMe and its phase I and II metabolites identified in HepaRG cell incubations together with their metabolic reactions, precursor ion mass (PI) recorded in MS^1, the corresponding characteristic fragment ions (FI) and their intensity in MS^2, the calculated exact masses, the corresponding elemental composition, the deviation of the measured from the calculated masses given as errors in ppm, the retention times (RT) in minutes (min), and the peak area. The metabolites were sorted by mass and RT.

Metabolite ID	Metabolic reaction	Characteristic ions' measured accurate masses, u	Relative intensity in MS^2, %	Calculated exact masses, *m/z*	Elemental composition	Error, ppm	RT, min	Peak area
Parent compound		PI at *m/z* 296.1637	33	PI at *m/z* 296.1638	$C_{19}H_{22}O_2N$	-0.34	5.70	2.04E+08
		FI at *m/z* 159.0803	2	FI at *m/z* 159.0801	$C_{11}H_{11}O$	1.26		
		FI at *m/z* 121.0649	100	FI at *m/z* 121.0645	C_8H_9O	3.30		
		FI at *m/z* 91.0547	12	FI at *m/z* 91.0540	C_7H_7	7.69		
M1	*O*-Dealkylation	PI at *m/z* 282.1483	80	PI at *m/z* 282.1482	$C_{18}H_{20}O_2N$	0.35	5.25	2.14E+04
		FI at *m/z* 176.1070	36	FI at *m/z* 176.1065	$C_{11}H_{14}ON$	2.84		
		FI at *m/z* 159.0804	100	FI at *m/z* 159.0801	$C_{11}H_{11}O$	1.89		
		FI at *m/z* 131.0492	44	FI at *m/z* 131.0489	C_9H_7O	2.29		
		FI at *m/z* 107.0495	98	FI at *m/z* 107.0489	C_7H_7O	5.60		
M2	*O*-Dealkylation + ring-opening + hydroxylation	PI at *m/z* 302.1748	34	PI at *m/z* 302.1743	$C_{18}H_{24}O_3N$	1.65	4.13	1.39E+05
		FI at *m/z* 284.1648	2	FI at *m/z* 284.1638	$C_{18}H_{22}O_2N$	3.52		
		FI at *m/z* 164.1069	6	FI at *m/z* 164.1065	$C_{10}H_{14}ON$	2.44		
		FI at *m/z* 121.0650	100	FI at *m/z* 121.0645	C_8H_9O	4.13		
		FI at *m/z* 91.0548	14	FI at *m/z* 91.0540	C_7H_7	8.79		
M3	Hydroxylation	PI at *m/z* 312.1587	19	PI at *m/z* 312.1587	$C_{19}H_{22}O_3N$	0.00	5.21	9.54E+05
		FI at *m/z* 159.0803	2	FI at *m/z* 159.0801	$C_{11}H_{11}O$	1.26		
		FI at *m/z* 137.0598	100	FI at *m/z* 137.0594	$C_8H_9O_2$	2.92		
		FI at *m/z* 107.0495	12	FI at *m/z* 107.0489	C_7H_7O	5.60		
M4	*O*-Dealkylation + ring-opening + carboxylation	PI at *m/z* 316.1541	100	PI at *m/z* 316.1536	$C_{18}H_{22O4}N$	1.58	4.00	2.31E+04
		FI at *m/z* 210.1124	62	FI at *m/z* 210.1119	$C_{11}H_{16}O_3N$	2.38		
		FI at *m/z* 193.0857	63	FI at *m/z* 193.0855	$C_{11}H_{13}O_3$	1.04		
		FI at *m/z* 175.0753	90	FI at *m/z* 175.0750	$C_{11}H_{11}O_2$	1.71		

		FI at *m/z* 147.0803	29	FI at *m/z* 147.0801	$C_{10}H_{11}O$	1.36		
		FI at *m/z* 107.0495	93	FI at *m/z* 107.0489	C_7H_7O	5.60		
M5	Ring-opening + hydroxylation	PI at *m/z* 316.1897	47	PI at *m/z* 316.1899	$C_{19}H_{26}O_3N$	-0.63	4.33	3.92E+06
		FI at *m/z* 299.1637	4	FI at *m/z* 299.1635	$C_{19}H_{23}O_3$	0.67		
		FI at *m/z* 281.1525	1	FI at *m/z* 281.1530	$C_{19}H_{21}O_2$	-1.78		
		FI at *m/z* 179.1065	7	FI at *m/z* 179.1062	$C_{11}H_{15}O_2$	1.67		
		FI at *m/z* 161.0958	7	FI at *m/z* 161.0957	$C_{11}H_{13}O$	0.62		
		FI at *m/z* 121.0650	100	FI at *m/z* 121.0645	C_8H_9O	4.13		
		FI at *m/z* 91.0547	13	FI at *m/z* 91.0540	C_7H_7	7.69		
M6	Dihydroxylation	PI at *m/z* 328.1539	14	PI at *m/z* 328.1536	$C_{19}H_{22}O_4N$	0.91	4.90	1.06E+03
		FI at *m/z* 310.1430	16	FI at *m/z* 310.1431	$C_{19}H_{20}O_3N$	-0.32		
		FI at *m/z* 137.0597	100	FI at *m/z* 137.0594	$C_8H_9O_2$	2.19		
		FI at *m/z* 107.0494	13	FI at *m/z* 107.0489	C_7H_7O	4.67		
M7	Ring-opening + carboxylation	PI at *m/z* 330.1695	38	PI at *m/z* 330.1692	$C_{19}H_{24}O_4N$	0.91	4.35	1.55E+06
		FI at *m/z* 313.1430	1	FI at *m/z* 313.1428	$C_{19}H_{21}O_4$	0.64		
		FI at *m/z* 295.1327	1	FI at *m/z* 295.1323	$C_{19}H_{19}O_3$	1.36		
		FI at *m/z* 175.0752	2	FI at *m/z* 175.0750	$C_{11}H_{11}O_2$	1.14		
		FI at *m/z* 147.0804	1	FI at *m/z* 147.0801	$C_{10}H_{11}O$	2.04		
		FI at *m/z* 121.0650	100	FI at *m/z* 121.0645	C_8H_9O	4.13		
		FI at *m/z* 91.0547	13	FI at *m/z* 91.0540	C_7H_7	7.69		
M8	Ring-opening + hydroxylation + glucuronidation	PI at *m/z* 492.2230	57	PI at *m/z* 492.2217	$C_{25}H_{34}O_9N$	2.64	3.74	9.78E+03
		FI at *m/z* 316.1905	4	FI at *m/z* 316.1899	$C_{19}H_{26}O_3N$	1.90		
		FI at *m/z* 299.1641	1	FI at *m/z* 299.1635	$C_{19}H_{22}O_3$	2.01		
		FI at *m/z* 179.1065	7	FI at *m/z* 179.1062	$C_{11}H_{15}O_2$	1.67		
		FI at *m/z* 121.0650	100	FI at *m/z* 121.0645	C_8H_9O	4.13		
		FI at *m/z* 91.0547	2	FI at *m/z* 91.0540	C_7H_7	7.69		

Table 1B: List of 2C-B-FLY-NB2EtO5Cl and its phase I and II metabolites identified in HepaRG cell incubations together with their metabolic reactions, precursor ion mass (PI) recorded in MS^1, the corresponding characteristic fragment ions (FI) and their intensity in MS^2, the calculated exact masses, the corresponding elemental composition, the deviation of the measured from the calculated masses given as errors in ppm, the retention times (RT) in minutes (min), and the peak area. The metabolites were sorted by mass and RT.

Metabolite ID	Metabolic reaction	Characteristic ions measured accurate masses, u	Relative intensity in MS^2, %	Calculated exact masses, *m/z*	Elemental composition	Error, ppm	RT, min	Peak area
Parent compound		PI at *m/z* 452.0626	58	PI at *m/z* 452.0614	$C_{21}H_{24}O_3NBrCl$	2.65	6.77	5.47E+08
		FI at *m/z* 267.0014	10	FI at *m/z* 267.0011	$C_{12}H_{12}O_2Br$	1.12		
		FI at *m/z* 188.0830	5	FI at *m/z* 188.0828	$C_{12}H_{12}O_2$	1.06		
		FI at *m/z* 169.0413	100	FI at *m/z* 169.0411	$C_9H_{10}OCl$	1.18		
		FI at *m/z* 141.0464	18	FI at *m/z* 141.0462	$C_8H_{10}Cl$	1.42		
M9	*O*-Dealkylation	PI at *m/z* 424.0306	70	PI at *m/z* 424.0302	$C_{19}H_{20}O_3NBrCl$	0.94	6.14	1.38E+07
		FI at *m/z* 267.0013	100	FI at *m/z* 267.0011	$C_{12}H_{12}O_2Br$	0.75		
		FI at *m/z* 188.0830	42	FI at *m/z* 188.0828	$C_{12}H_{12}O_2$	1.06		
		FI at *m/z* 141.0100	33	FI at *m/z* 141.0099	C_7H_6OCl	0.71		
M10	Hydroxylation isomer 1	PI at *m/z* 468.0574	54	PI at *m/z* 468.0563	$C_{21}H_{24}O_4NBrCl$	2.35	5.74	2.37E+07
		FI at *m/z* 450.0466	2	FI at *m/z* 450.0458	$C_{21}H_{22}O_3NBrCl$	1.78		
		FI at *m/z* 264.9857	6	FI at *m/z* 264.9855	$C_{12}H_{10}O_2Br$	0.75		
		FI at *m/z* 186.0676	4	FI at *m/z* 186.0672	$C_{12}H_{10}O_2$	2.15		
		FI at *m/z* 169.0413	100	FI at *m/z* 169.0411	$C_9H_{10}OCl$	1.18		
		FI at *m/z* 141.0465	17	FI at *m/z* 141.0462	$C_8H_{10}Cl$	2.13		
M11	Hydroxylation isomer 2	PI at *m/z* 468.0573	7	PI at *m/z* 468.0563	$C_{21}H_{24}O_4NBrCl$	2.14	6.40	1.51E+08
		FI at *m/z* 450.0461	100	FI at *m/z* 450.0458	$C_{21}H_{22}O_3NBrCl$	0.67		
		FI at *m/z* 267.0011	47	FI at *m/z* 267.0011	$C_{12}H_{12}O_2Br$	0		
		FI at *m/z* 188.0831	32	FI at *m/z* 188.0828	$C_{12}H_{12}O_2$	1.60		
		FI at *m/z* 169.0414	95	FI at *m/z* 169.0411	$C_9H_{10}OCl$	1.77		
		FI at *m/z* 141.0464	12	FI at *m/z* 141.0462	$C_8H_{10}Cl$	1.42		
M12	Dihydroxylation	PI at *m/z* 484.0522	7	PI at *m/z* 484.0512	$C_{21}H_{24}O_5NBrCl$	2.07	5.27	1.77E+07

		FI at *m/z* 466.0411	56	FI at *m/z* 466.0407	$C_{21}H_{22}O_4NBrCl$	0.86		
		FI at *m/z* 448.0304	6	FI at *m/z* 448.0302	$C_{21}H_{20}O_3NBrCl$	0.45		
		FI at *m/z* 264.9858	11	FI at *m/z* 264.9855	$C_{12}H_{10}O_2Br$	1.13		
		FI at *m/z* 186.0675	17	FI at *m/z* 186.0672	$C_{12}H_{10}O_2$	1.61		
		FI at *m/z* 169.0414	100	FI at *m/z* 169.0411	$C_9H_{10}OCl$	1.77		
		FI at *m/z* 141.0465	11	FI at *m/z* 141.0462	$C_8H_{10}Cl$	2.13		
M13	*O*-Dealkylation + hydroxylation + glucuronidation	PI at *m/z* 616.0583	83	PI at *m/z* 616.0569	$C_{25}H_{28}O_{10}NBrCl$	2.27	4.77	9.68E+04
		FI at *m/z* 440.0267	1	FI at *m/z* 440.0251	$C_{19}H_{20}O_4NBrCl$	3.64		
		FI at *m/z* 422.0154	41	FI at *m/z* 422.0146	$C_{19}H_{18}O_3NBrCl$	1.90		
		FI at *m/z* 264.9856	100	FI at *m/z* 264.9855	$C_{12}H_{10}O_2Br$	0.38		
		FI at *m/z* 186.0678	18	FI at *m/z* 186.0672	$C_{12}H_{10}O_2$	3.22		
		FI at *m/z* 141.0101	94	FI at *m/z* 141.0099	C_7H_6OCl	1.42		
M14	Hydroxylation + glucuronidation	PI at *m/z* 644.0880	7	PI at *m/z* 644.0881	$C_{27}H_{32}O_{10}NBrCl$	-0.16	5.26	3.80E+06
		FI at *m/z* 468.0573	45	FI at *m/z* 468.0563	$C_{21}H_{24}O_4NBrCl$	2.14		
		FI at *m/z* 450.0471	26	FI at *m/z* 450.0458	$C_{21}H_{22}O_3NBrCl$	2.89		
		FI at *m/z* 264.9864	6	FI at *m/z* 264.9855	$C_{12}H_{10}O_2Br$	3.40		
		FI at *m/z* 186.0679	4	FI at *m/z* 186.0672	$C_{12}H_{10}O_2$	3.76		
		FI at *m/z* 169.0413	100	FI at *m/z* 169.0411	$C_9H_{10}OCl$	1.18		
		FI at *m/z* 141.0465	14	FI at *m/z* 141.0462	$C_8H_{10}Cl$	2.13		

Table 1C. List of 2C-B-FLY-NBOMe and its phase I and II metabolites identified in HepaRG cell incubations together with their metabolic reactions, precursor ion mass (PI) recorded in MS^1, the corresponding characteristic fragment ions (FI) and their intensity in MS^2, the calculated exact masses, the corresponding elemental composition, the deviation of the measured from the calculated masses given as errors in ppm, the retention times (RT) in minutes (min), and the peak area. The metabolites were sorted by mass and RT.

Metabolite ID	Metabolic reaction	Characteristic ions measured accurate masses, u	Relative intensity in MS^2, %	Calculated exact masses, *m/z*	Elemental composition	Error, ppm	RT, min	Peak area
Parent compound		PI at *m/z* 404.0843	41	PI at *m/z* 404.0848	$C_{20}H_{23}O_3NBr$	-0.49	6.05	4.21E+08
		FI at *m/z* 325.1668	2	FI at *m/z* 325.1665	$C_{20}H_{23}O_3N$	0.92		
		FI at *m/z* 267.0008	3	FI at *m/z* 267.0011	$C_{12}H_{12}O_2Br$	-1.12		
		FI at *m/z* 188.0829	1	FI at *m/z* 188.0828	$C_{12}H_{12}O_2$	0.53		
		FI at *m/z* 121.0649	100	FI at *m/z* 121.0645	C_8H_9O	3.30		
		FI at *m/z* 91.0547	21	FI at *m/z* 91.0540	C_7H_7	7.69		
M15	*O*-Dealkylation	PI at *m/z* 390.0696	89	PI at *m/z* 390.0692	$C_{19}H_{21}O_3NBr$	1.03	5.69	5.48E+07
		FI at *m/z* 267.0010	100	FI at *m/z* 267.0011	$C_{12}H_{12}O_2Br$	-0.37		
		FI at *m/z* 188.0834	32	FI at *m/z* 188.0828	$C_{12}H_{12}O_2$	3.19		
		FI at *m/z* 107.0495	78	FI at *m/z* 107.0489	C_7H_7O	5.60		
M16	*O*-Dealkylation + hydroxylation	PI at *m/z* 406.0635	27	PI at *m/z* 406.0641	$C_{19}H_{21}O_4NBr$	-1.48	4.48	1.03E+04
		FI at *m/z* 388.0530	65	FI at *m/z* 388.0536	$C_{19}H_{19}O_3NBr$	-1.55		
		FI at *m/z* 300.0223	3	FI at *m/z* 300.0224	$C_{12}H_{14}O_3NBr$	-0.33		
		FI at *m/z* 264.9851	100	FI at *m/z* 264.9855	$C_{12}H_{10}O_2Br$	-1.51		
		FI at *m/z* 186.0672	31	FI at *m/z* 186.0672	$C_{12}H_{10}O_2$	0		
		FI at *m/z* 107.0494	95	FI at *m/z* 107.0489	C_7H_7O	4.67		
M17	Hydroxylation isomer 1	PI at *m/z* 420.0797	43	PI at *m/z* 420.0797	$C_{20}H_{23}O_4NBr$	0	4.96	2.50E+09
		FI at *m/z* 264.9851	5	FI at *m/z* 264.9855	$C_{12}H_{10}O_2Br$	-1.51		
		FI at *m/z* 186.0673	2	FI at *m/z* 186.0672	$C_{12}H_{10}O_2$	0.54		
		FI at *m/z* 121.0650	100	FI at *m/z* 121.0645	C_8H_9O	4.13		
		FI at *m/z* 91.0547	22	FI at *m/z* 91.0540	C_7H_7	7.69		
M18	Hydroxylation isomer 2	PI at *m/z* 420.0792	7	PI at *m/z* 420.0797	$C_{20}H_{23}O_4NBr$	-1.19	5.86	1.61E+07

		FI at *m/z* 402.0692	96	FI at *m/z* 402.0692	$C_{20}H_{21}O_3NBr$	0		
		FI at *m/z* 267.0009	43	FI at *m/z* 267.0011	$C_{12}H_{12}O_2Br$	-0.75		
		FI at *m/z* 188.0828	27	FI at *m/z* 188.0828	$C_{12}H_{12}O_2$	0		
		FI at *m/z* 121.0648	100	FI at *m/z* 121.0645	C_8H_9O	2.48		
		FI at *m/z* 91.0546	14	FI at *m/z* 91.0540	C_7H_7	6.59		
M19	Dihydroxylation	PI at *m/z* 436.0745	27	PI at *m/z* 436.0746	$C_{20}H_{23}O_5NBr$	-0.23	4.74	1.97E+06
		FI at *m/z* 418.0638	25	FI at *m/z* 418.0641	$C_{20}H_{21}O_4NBr$	-0.72		
		FI at *m/z* 400.0577	3	FI at *m/z* 400.0536	$C_{20}H_{19}O_3NBr$	-2.25		
		FI at *m/z* 264.9850	4	FI at *m/z* 264.9855	$C_{12}H_{10}O_2Br$	-1.89		
		FI at *m/z* 186.0671	5	FI at *m/z* 186.0672	$C_{12}H_{10}O_2$	-0.54		
		FI at *m/z* 121.0648	100	FI at *m/z* 121.0645	C_8H_9O	2.48		
		FI at *m/z* 91.0546	17	FI at *m/z* 91.0540	C_7H_7	6.59		
M20	*O*-Dealkylation + glucuronidation	PI at *m/z* 566.1003	76	PI at *m/z* 566.1010	$C_{25}H_{29}O_9NBr$	-1.24 –	5.32	2.91E+04
		FI at *m/z* 390.0682	28	FI at *m/z* 390.0692	$C_{19}H_{21}O_3NBr$	2.56 -		
		FI at *m/z* 267.0006	52	FI at *m/z* 267.0011	$C_{12}H_{12}O_2Br$	1.87		
		FI at *m/z* 188.0831	1	FI at *m/z* 188.0828	$C_{12}H_{12}O_2$	1.60		
		FI at *m/z* 107.0493	100	FI at *m/z* 107.0489	C_7H_7O	3.74		

Table 2. Results of the monooxygenases activity screening

Metabolite ID	Investigated NPS	Metabolic reaction	Isoenzymes
M1	5-APB-NBOMe	*O*-Dealkylation	CYP1A2
M3	5-APB-NBOMe	Hydroxylation	CYP1A2, 2D6, 2C8
M9	2C-B-FLY-NB2EtO5Cl	*O*-Dealkylation	CYP1A2, 2C19, 3A4
M10	2C-B-FLY-NB2EtO5Cl	Hydroxylation isomer 1	CYP2C19, 3A4
M11	2C-B-FLY-NB2EtO5Cl	Hydroxylation isomer 2	CYP2C19, 2D6, 3A4
M15	2C-B-FLY-NBOMe	*O*-Dealkylation	CYP1A2, 2C8
M17	2C-B-FLY-NBOMe	Hydroxylation isomer 1	CYP1A2, 2C8, 2D6
M19	2C-B-FLY-NBOMe	Hydroxylation isomer 2	CYP1A2

Table 3. Results of the UDP-glucuronyltransferase activity screening

Metabolite ID	Investigated NBOMe	Metabolic reaction	Isoenzymes
M13	2C-B-FLY-NB2EtO5Cl	*O*-Dealkylation + hydroxylation + glucuronidation	UGT1A7, 1A9
M14	2C-B-FLY-NB2EtO5Cl	hydroxylation + glucuronidation	UGT1A9
M20	2C-B-FLY-NBOMe	*O*-Dealkylation + glucuronidation	UGT1A9

Table 4. Determined plasma protein binding (PPB) of 5-APB-NBOMe, 2C-B-FLY-NB2EtO5Cl, and 2C-B-FLY-NBOMe at three different concentrations (1, 2.5, and 5 µM) and their calculated logP values.

Compound	Concentration, µM	PPB, %	logP
5-APB-NBOMe	1	86	4.3
	2.5	89	
	5	93	
2C-B-FLY-NB2EtO5Cl	1	87	5.3
	2.5	99	
	5	99	
2C-B-FLY-NBOMe	1	91	4.1
	2.5	96	
	5	97	

Table 5.

List of compounds detected or identified by LC-MS^n standard urine screening approach after administration of 0.02 or 0.2 mg/kg body weight in rat urine together with their metabolic reaction, precursor ion mass (PI) recorded in MS^1, the corresponding characteristic fragment ions (FI) in MS^2, PI recorded in MS^2, the corresponding characteristic FI in MS^3, their relative intensities and the retention times (RT) in minutes (min).

Metabolite ID	Metabolic reaction	Rat urine 0.02 mg/kg BW	Rat urine 0.2 mg/kg BW	Characteristic MS^2 fragment ions, *m/z*	Relative intensity in MS^2, %	Characteristic MS^3 fragment ions, *m/z*	Relative intensity in MS^3, %	RT, min
M5	Ring-Opening + hydroxylation	I	I	PI at *m/z* 316	0	PI at *m/z* 121	0	8.95
				FI at *m/z* 191	21	FI at *m/z* 93	100	
				FI at *m/z* 179	42	FI at *m/z* 91	26	
				FI at *m/z* 173	31			
				FI at *m/z* 161	18			
				FI at *m/z* 121	100			
M8	Ring-Opening + carboxylation	I	I	PI at *m/z* 330	0	PI at *m/z* 121	0	8.64
				FI at *m/z* 295	11	FI at *m/z* 93	100	
				FI at *m/z* 285	32	FI at *m/z* 91	24	
				FI at *m/z* 208	11			
				FI at *m/z* 187	6			
				FI at *m/z* 121	100			
M17	Hydroxylation isomer 1	D	D	PI at *m/z* 420	0	PI at *m/z* 385	0	6.84
				FI at *m/z* 385	100	FI at *m/z* 209	64	
				FI at *m/z* 384	29	FI at *m/z* 191	53	
				FI at *m/z* 209	28	FI at *m/z* 173	100	
				FI at *m/z* 191	25	FI at *m/z* 146	8	
				FI at *m/z* 173	22	FI at *m/z* 133	92	